arXiv:1507.02541v1 [hep-ph] 9 Jul 2015

Leptonic Decay Constant of ρ at Physical Point

Ying Chen,[1*] Andrei Alexandru,[2] Terrence Draper,[3] Keh-Fei Liu,[3] Zhaofeng Liu,[1] and Yi-Bo Yang[3]
[1] *Institute of High Energy Physics and Theoretical Physics Center for Science Facilities,*
Chinese Academy of Sciences, Beijing 100049, People's Republic of China
[2] *Department of Physics, George Washington University, Washington, DC 20052, USA*
[3] *Department of Physics and Astronomy, University of Kentucky, Lexington, KY 40506, USA*

The ρ meson leptonic decay constant at the physical pion mass is calculated with chiral fermions. Overlap valence quarks are used on the $L^3 \times T = 48^3 \times 96$ $N_f = 2+1$ domain-wall fermion configurations with light sea quarks at the physical point and the spatial extension of 5.5 fm. The mass of the vector meson ρ is determined to be $m_\rho = 775.9 \pm 6.0 \pm 1.8$ MeV, and the valence $\pi\rho$ sigma term is extracted to be $\sigma_{\pi\rho}^{(\rm val)} = 9.82(6)$ MeV from Feynmann-Hellman theorem. By adopting a new method to reduce the noise of the wall-wall correlation functions of hadrons, we obtain the ρ leptonic decay constant $f_\rho = 208.5 \pm 5.5 \pm 0.9$ MeV, which is in very good agreement with the experimental value $f_\rho = 209.4 \pm 1.5$ MeV derived from the τ decay $\tau \to \rho\nu_\tau$.

PACS numbers: 12.38.Gc, 13.20.Jf, 14.40.Be, 12.39.Fe.

The standard quantities that are used to test lattice QCD against experiments include hadron masses, pseudoscalar meson decay constants f_π and f_K, and B_K [1]. On the other hand, the lattice results are getting precise enough, such as f_{D_s} [2, 3], so that any significant deviation from experiments could be taken as a signal for physics beyond the standard model. Now that lattice configurations with $N_f = 2+1$ flavors are available for physical pion mass and large volume, the list of physical observables should be expanded to have a broader examination of lattice calculations against experiments. The obvious choices include the vector meson decay constants for ρ, K^*, D^* and D_s^* and the vector to pseudoscalar radiative decays $V \to P\gamma$, etc. In this work we shall report our analysis of the leptonic decay constant $f_{\rho^\pm}$ of the charged ρ meson, which describes the coupling of $\rho^\pm$ and lepton pair $l\bar{\nu}$ through the charged weak current interaction.

Gauge configurations of $N_f = 2+1$ domain-wall fermions with large spatial volume and physical pion mass have been generated by the RBC & UKQCD Collaborations [1]. This work is based on the 48I gauge ensemble with lattice size $L^3 \times T = 48^3 \times 96$ [1]. The lattice spacing has been determined to be $a^{-1} = 1.730(4)$ GeV, such that the spatial extension of the lattice is approximately $La \sim 5.5$ fm. The light sea quark mass is set to give the pion mass $m_\pi^{(\rm sea)} = 139.2(4)$ MeV. For the valence quarks, we adopt the overlap fermion action, which is another realization of the chiral fermions on the lattice. The low-energy constant $\Delta_{\rm mix}$, which measures the mismatch of the mixed valence and sea pion masses between the domain-wall fermion and the overlap fermion, is shown to be very small [4]. Since overlap fermion accommodates the multi-mass algorithm and the eigenvectors are the same for different quark masses, we use 1000 pairs of eigenvectors plus the zero modes for deflation in calculating quark propagators for several masses on 45 configurations (see Ref [5] for details). The bare mass parameters are chosen as $am_q^{(\rm val)} = 0.00170, 0.00240, 0.00300, 0.00455, 0.00600$ and 0.02030, which give the pion mass ranging from 114 to 371 MeV. In this way we can discern the chiral behaviors of the mass and the leptonic decay width of the ρ meson.

TABLE I: The table lists the pion masses m_π, the pion decay constants f_π, and the masses of ρ at different bare valence quark masses.

$am_q^{(\rm val)}$	0.00170	0.00240	0.00300	0.00455	0.00600	0.02030
m_π(MeV)	114(2)	135(2)	149(2)	182(2)	208(2)	371(1)
f_π(MeV)	130.3(9)	131.0(9)	131.6(8))	...	...	...
m_ρ(MeV)	773(7)	775(6)	779(6)	784(5)	789(5)	836(3)

We first extract the decay constant of pion according to the partially conserved axial current relation

$$m_\pi^2 f_\pi = (m_u + m_d)\langle 0|\bar{u}\gamma_5 d|\pi\rangle. \tag{1}$$

For overlap fermions, the quark mass renormalization constant Z_m and the renormalization constant Z_P of the psuedoscalar density $\bar{u}\gamma_5 d$ satisfy the relation $Z_m Z_P = 1$. Thus the calculation of f_π can be carried out straightforwardly by taking $m_u = m_d = m_q^{(\rm val)}$ after the matrix element in Eq. (1) is obtained from the $\langle A_4 P\rangle$ and $\langle PP\rangle$ correlation functions. The pion masses and decay constants are listed in Table I. Since the pion masses are very close to the physical pion mass, we perform simply a linear interpolation in m_π^2 and get $f_\pi = 131.3(6)$ MeV at the physical pion mass $m_\pi = 139.5$ MeV, which agrees with RBC&UKQCD's result $f_\pi = 131.1(3)$ MeV on the same lattice and their final theoretical prediction $f_\pi = 130.2(9)$ MeV [1]. RBC&UKQCD also calculates f_π on a larger lattice with a smaller lattice spacing, $a^{-1} = 2.359(7)$ GeV, with a result $f_\pi = 130.9(4)$ MeV. Their f_πs on the two lattices imply very small finite a artifacts. This comparison can be taken as a calibration of our formalism.

---

[*] cheny@ihep.ac.cn

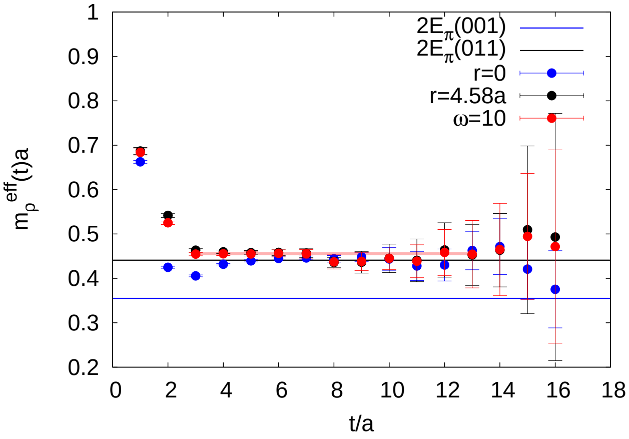

FIG. 1: The effective mass plateaus of ρ at $m_\pi = 208(2)$ MeV. The blue and black points are from the correlation functions $C(r=0,t)$ and $C(r=4.58a,t)$, respectively. The red points are from the mixed correlation function $C^\omega(t) = C(0,t) + \omega C(4.58a,t)$ with the mixing parameter $\omega = 10$. The red band shows the fitted mass in the time range $t/a \in [3,13]$. The blue line and the black line are the energies of two non-interacting pions $2E_\pi$ with the momentum modes $\mathbf{p}a = 2\pi/L(0,0,\pm1)$ and $\mathbf{p}a = 2\pi/L(0,\pm1,\pm1)$, respectively.

When calculating the two-point functions in the vector channel, we first perform Coulomb gauge fixing on the 45 gauge configurations. The quark propagators are computed using a wall source, thus the source operators of the vector can be expressed as

$$O_{V,i}^{(\mathrm{w})}(t) = \sum_{\mathbf{y},\mathbf{z}} \bar{u}(\mathbf{y},t)\gamma_i d(\mathbf{z},t). \tag{2}$$

For the sink operators of the vector, we use the spatially extended operators $O_{V,i}(\mathbf{x},t;\mathbf{r})$ by splitting the quark and antiquark field operator with different spatial displacements $\mathbf{r}$, namely, $O_{V,i}(\mathbf{x},t;\mathbf{r}) = \bar{u}(\mathbf{x},t)\gamma_i d(\mathbf{x}+\mathbf{r},t)$. Subsequently the two-point functions $C(t,r)$ with different spatial separation r are calculated as

$$C(r,t) = \frac{1}{3N_r} \sum_{\mathbf{x},i,|\mathbf{r}|=r} \langle 0|O_{V,i}(\mathbf{x},t;\mathbf{r})O_{V,i}^{(\mathrm{w})\dagger}(0)|0\rangle, \tag{3}$$

where N_r is the number of $\mathbf{r}$s that satisfy $|\mathbf{r}| = r$. The effective mass plateaus of $C(r,t)$ with $r = 0$ (blue points) and $r = \sqrt{20}a = 4.58a$(black points) at $m_\pi = 208(2)$ MeV are plotted in Fig. 1. It is seen that the plateaus are converged to a uniform effective mass in large time range. The difference of the plateaus in the short time range shows the r-dependence of the contamination from higher states. In order to reduce the higher state contamination, we linearly combine the two correlation functions as $C_{\mathrm{mix}}(t) = C(0,t) + \omega C(4.58a,t)$ with an optimal mixing parameter $\omega = 10$, by which we can get a very flat effective mass plateau starting from $t/a = 3$, as shown in the figure (red points). We fit $C_{\mathrm{mix}}(t)$ using a single-exponential form in the time range $t/a \in [3,13]$ and get $m_V a = 0.456(4)$ (plotted as a red band), where the error is statistical and is obtained through a jackknife analysis.

Through the large N_c analysis, it is suggested by Jaffe [6] that the ρ meson is an *ordinary* meson like the Feshbach resonance which exists as a confined $q\bar{q}$ state in the continuum with zero width in the large N_c limit. Its Breit-Wigner width manifests the coupling of the bound state and the scattering $\pi\pi$ states, which vanishes as N_c goes to infinity, while its pole mass is insensitive to the strength of the coupling [7]. In the continuum, the resonance parameters of ρ, $m_\rho = 775$ MeV and $\Gamma_\rho \approx 150$ MeV, have been extracted in the $I = 1$ $\pi\pi$ scattering channel. On a finite lattice, the eigenstates of the QCD Hamiltonian in the ρ channel are actually the superpositions of the discretized interacting $\pi\pi$ scattering states and the would-be $q\bar{q}$ confined state, and the energy shifts of these eigenstates from the interacting $\pi\pi$ states or the $q\bar{q}$ state encode the resonance properties. Many lattice calculations [8–11] have been carried out to extract the resonance parameters of ρ according to the Lüscher method [12]. It is known that the lattice spectrum in the ρ channel should show an avoided level crossing behavior when the energy of $\pi\pi$ states approaches to the mass of the resonance by varying the lattice size or the relative momentum of the $\pi\pi$ states, and the mixing of the would-be $q\bar{q}$ confined state and the nearby scattering state gives two eigenstates. For the spatial extension $La \sim 5.5$ fm of our lattice and in the case of $m_\pi = 208$ MeV, the two lowest energy thresholds of the $P-$ wave $\pi\pi$ states are $2E_\pi(001) = 614$ MeV (shown in Fig. 1 as a blue line) and $2E_\pi(011) = 761$ MeV (shown in Fig. 1 as a black line) with the relative momenta $\mathbf{p}a = 2\pi/L(0,0,\pm1)$ and $\mathbf{p}a = 2\pi/L(0,\pm1,\pm1)$, respectively. Since $2E_\pi(001)$ is far from the expected ρ mass, the corresponding $\pi\pi$ state should mix little with ρ and therefore have an energy close to $2E_\pi(001)$, but we do not observe this state in the vector correlation function. The reason for its absence might be due to the implementation of the Coulomb wall-source operator which suppresses the scattering states with non-zero relative momenta (we will discuss this in depth in another publication). However, $2E_\pi(011)$ is very close to the expected ρ mass, so the mixing of the corresponding $\pi\pi$ state and the $q\bar{q}$ state can be sizable. According to the feature of the avoided level crossing, the mixing gives two states with nearly degenerate energies around m_ρ, which, however, cannot be resolved in our analysis. In this sense, we expect that the plateau in Fig. 1 illustrates the effective energy of the two adjacent states, and will take the fitted energy value $m_V a = 0.456(4)$ as an approximation of the ρ mass in the lattice unit.

We take a similar analysis procedure for the correlation functions at other pion masses, and the extracted masses of ρ are listed in Table I and are also plotted in Fig. 2 with respect to m_π^2, by which the chiral behavior of m_ρ can be investigated. A new chiral extrapolation formula based on a modified $\overline{MS}$ regulator and a power counting scheme [13] gives $m_\rho(m_\pi) = m_\rho(0) + c_1 m_\pi^2 + c_2 m_\pi^3 +$

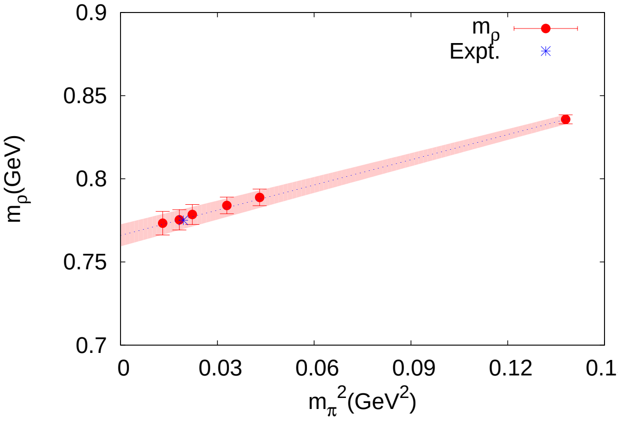

FIG. 2: The ρ mass $m_\rho = 775.9 \pm 6.0$ MeV at the physical point is interpolated by $m_\rho(m_\pi) = m_\rho(0) + c_1 m_\pi^2$. The red band shows the error of the interpolation. The experimental value of $m_\rho = 775$ MeV is also plotted for comparison.

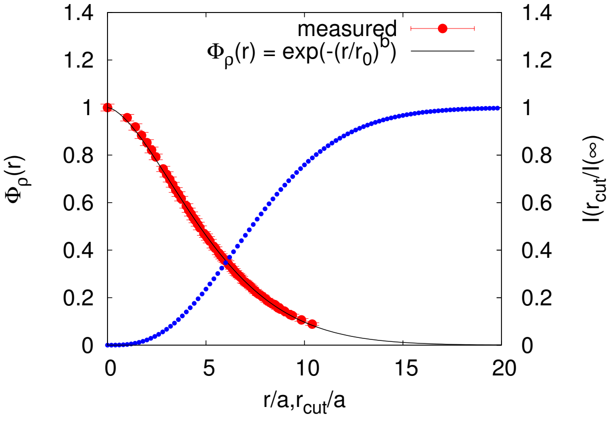

FIG. 3: The red points show $\Phi_i(r)$ which depicts the fall-off of $C(r,t)$ when r increases. The parameterization of $\Phi_i(r)$ is plotted by the curve. The blue points are the ratios $I_1(r_c)/I(\infty)$ at different r_c.

$c_3 m_\pi^4 \ln \frac{m_\pi^2}{m_\rho^2}$, where the log term is due to self energy. However, from Fig. 2 it is seen that m_ρ is very linear in m_π^2 for m_π ranging from 114 MeV to 371 MeV. A correlated jackknife analysis using the form

$$m_\rho(m_\pi) = m_\rho(0) + c_1 m_\pi^2, \tag{4}$$

gives $m_\rho(0) = 766(7)$ MeV and $c_1 = 0.505(3)\,\mathrm{GeV}^{-1}$ with $\chi^2/d.o.f = 0.13$. The ρ mass at the physical m_π is $m_\rho = 775.9 \pm 6.0 \pm 1.8$ MeV, where the second error is due to the 0.23% uncertainty of the lattice spacing. Our data cannot discern higher order terms in m_π. We would like to point out that our study is carried out for the first time in the chiral region around the physical point and with chiral fermions, although there have been many lattice studies on this topic [14–17]. We note that c_1 is precisely determined, and serves potentially as a constraint on the chiral perturbation study of ρ. Furthermore, c_1 is exactly the valence or connected insertion part of the $\pi\rho$ sigma term from the Feynman-Hellman theorem $\sigma_{\pi\rho}^{(\mathrm{val})} = m_\pi^2\, dm_\rho/dm_\pi^2 = c_1 m_\pi^2$, since the sea is fixed in our partially quenched calculation of m_ρ. One can determine the disconnected part from a direct calculation of the $m\bar{\psi}\psi$ matrix element in the disconnected three-point correlator. From the fitted c_1 in Eq. (4), we find $\sigma_{\pi\rho}^{(\mathrm{val})} = 9.82(6)$ MeV.

The leptonic decay constant f_ρ is also an important characteristic quantity of ρ. Most of previous lattice studies on f_ρ were performed at relatively heavy pion masses [18–22]. Here we would like to extract the decay constant of charged ρ at the physical point. For charged ρ, for example, ρ^-, f_{ρ^-} is defined by

$$\langle 0|J_\mu^{(-)}(0)|\rho^-(\vec{p},\zeta)\rangle = m_\rho f_{\rho^-} \epsilon_\mu(\vec{p},\zeta), \tag{5}$$

where $J_\mu^{(-)}(x) = (\bar{u}\gamma_\mu d)(x)$ is the charged vector current and $\epsilon_\mu(\vec{p},\zeta)$ is the ζ-th polarization vector of ρ^- with $\zeta = 1, 2, 3$.

The spatial components of $J_\mu^{(-)}(x)$ are actually the operators $O_{V,i}(x;\mathbf{r}=0)$; therefore, the matrix element defined in Eq. (5) can be extracted from $C(r=0,t)$. The key challenge is to divide out the matrix element of the wall source operator $\langle 0|O_{V,i}^{(\mathrm{w})}|V(\vec{p},\zeta)\rangle$. Usually this matrix element can be derived by calculating the wall-wall correlation function

$$\begin{aligned} C^{(\mathrm{w})}(t) \;&\equiv\; \sum_r N_r C(r,t) = \frac{1}{3}\sum_i \langle 0|O_{V,i}^{(\mathrm{w})}(t) O_{V,i}^{(\mathrm{w}),\dagger}(0)|0\rangle \\ &=\; \frac{1}{3}\sum_{\mathbf{x},\mathbf{r},i} \langle 0|O_{V,i}(\mathbf{x},t;\mathbf{r}) O_{V,i}^{(\mathrm{w}),\dagger}(0)|0\rangle, \end{aligned} \tag{6}$$

where the last equation uses the definition of $C(r,t)$ in Eq. (3). However, a very large statistics is required to obtain a satisfactory signal-to-noise ratio for this kind of correlation function. The reason for noisy $C^{(\mathrm{w})}(t)$ is analyzed as follows. Using the spectral expression $C(r,t) = \sum_i \Phi_n(r) e^{-E_n t}$, when $t \to \infty$ one has

$$C^{(w)}(t) \;\approx\; \sum_r N_r \Phi_1(r) e^{-E_1 t} \tag{7}$$

In practice, we calculate $C(r,t)$ for r ranging from 0 to $10a$ and observe the profile of $\Phi_1(r)$ for $t = 7a$ where all $C(r,t)$ are almost saturated by the ground state. The $\Phi_1(r)$ at $m_\pi = 208(2)$ MeV (normalized as $\Phi_1(0) = 1$) is plotted in Fig. 3 as red points. It is seen that $\Phi_1(r)$ damps rapidly with r and can be parameterized as

$$\Phi_1(r) = \Phi_1(0) e^{-\left(\frac{r}{r_0}\right)^\alpha}, \tag{8}$$

with the parameters $\alpha = 1.60$ and $r_0 = 5.88a$. The curve illustrates this parameterization in the figure. We check

TABLE II: The renormalization constant Z_A obtained at different pion masses, which also gives Z_V by the relation $Z_A = Z_V$ for overlap fermions. The renormalized decay constants f_ρ are also listed in the table.

m_π(MeV)	114(2)	135(2)	149(2)	182(2)	208(2)	371(1)
Z_A	1.103(4)	1.103(3)	1.104(2)	1.104(2)	1.105(1)	1.105(1)
f_ρ(MeV)	206(7)	208(7)	211(6)	215(5)	217(5)	223(3)

this at other pion masses and find $\Phi_1(r)$ is similar for all the cases and is very insensitive to m_π. This means that when calculating the wall-to-wall correlation function $C^{(\mathrm{w})}(t)$, the $C(r,t)$s (see in Eq. (6)) with very large r contribute only noise and make $C^{(\mathrm{w})}(t)$ very noisy. In order to circumvent this difficulty, we introduce a cutoff r_c to exclude the contribute of $C(r,t)$s with $r > r_c$ from $C^{(\mathrm{w})}(t)$ and use the correlation function

$$C^{(\mathrm{w})}(r_c,t) = \sum_{r\leq r_c} N_r C(r,t), \tag{9}$$

to approximate $C^{(\mathrm{w})}(t)$. Letting $I_1(r') = \int_0^{r'} dr r^2 \Phi_1(r)$, one can see that the ratio $C^{(\mathrm{w})}(r_c,t)/C^{(\mathrm{w})}(t)$ can be depicted by the ratio $I_1(r_c)/I_1(\infty)$ at large t. The ratio $I_1(r_c)/I_1(\infty)$ using the parameterization above is also plotted in Fig. 3. It approaches to 1 beyond $r_c = 15a$ and is equal to 0.995 at $r_c = 20a$, whose deviation from one is already much smaller than the statistical error. So we take $C^{(\mathrm{w})}(20a,t)$ as a satisfactory approximation of $C^{(\mathrm{w})}$ throughout this work.

With this prescription, we carry out the joint fit to the correlation functions

$$\begin{aligned} C(0,t) &= \sum_n 2m_n L^3 f_n Z_n^{(\mathrm{w})} e^{-m_n t} \\ C^{(\mathrm{w})}(20a,t) &\approx \sum_n 2m_n L^3 (Z_n^{(\mathrm{w})})^2 e^{-m_n t}, \end{aligned} \tag{10}$$

where $Z_n^{(\mathrm{w})}$ is the matrix element of the wall source operator between the vacuum and the n-th state, and f_n is the bare decay constant of the n-th state according to the definition in Eq. (5). In practice, two exponentials are used in the fit and f_1 is taken as the bare decay constant of ρ (the second term is introduced to account for the contamination of higher states). Since f_1 is sensitive to the value of m_1, we adopt the single-elimination jackknife analysis procedure as follows. On each jackknife re-sampled ensemble, we first obtain the mass parameter m_1 from $C_{\mathrm{mix}}(t)$ defined previously, and then extract f_1 through a joint fit to Eq. (10) with m_1 fixed. After that, we quote the jackknife error of f_1 as the statistical error.

For the overlap fermion, the chiral symmetry dictates that $Z_V = Z_A$ for the local currents and it has been verified in the non-perturbative renormalization [23]. We have calculated Z_A from the Ward identity for a few bare quark masses and they are listed in Table II, where one can see that the quark mass dependence of Z_A is mild and the chiral limit value is $Z_A = 1.1045(8)$.

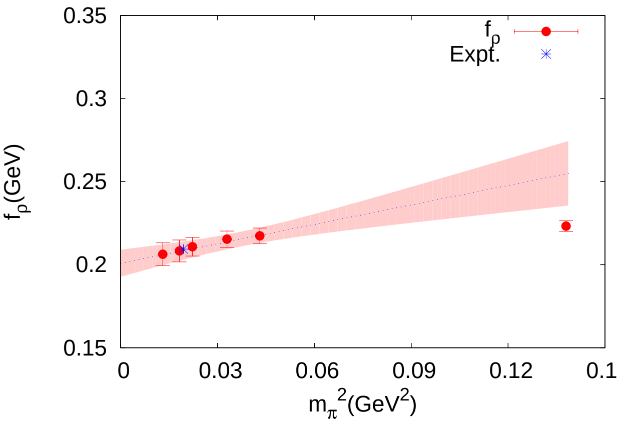

FIG. 4: The decay constant f_ρ obtained at different pion masses. The curve shows the linear interpolation in terms of m_π^2. The $f_{\rho^\pm}^{(exp)}$ extracted from the τ leptonic decay is also plotted as an asterisk.

From $Z_V = Z_A$ and the bare decay constant f_1, the renormalized decay constant f_ρ is obtained at different m_π, as illustrated in Fig. 4, where one can see that f_ρ is not linear in m_π^2 throughout the pion mass range. Fortunately, we have several m_πs very close to the physical pion mass, which facilitate us to do an linear interpolation in m_π^2 in the neighborhood of the physical pion mass. The final result of f_ρ at the physical point is

$$f_{\rho^\pm} = 208.5 \pm 5.5 \pm 0.9 \ \text{MeV}, \tag{11}$$

where the first error is statistical and the second is the combined uncertainty of Z_V, the scale parameter a^{-1}, and the approximated wall-wall correlation function.

Experimentally, $f_{\rho^\pm}$ can be derived from the branching ratio of τ lepton decaying into $\rho^-\nu_\tau$,

$$\mathrm{Br} = \frac{G_F^2 m_\tau |V_{ud}|^2}{8\pi} \tau_\tau m_\rho^2 f_{\rho^-}^2 \left(1 + \frac{m_\tau^2}{2m_\rho^2}\right)\left(1 - \frac{m_\rho^2}{m_\tau^2}\right)^2. \tag{12}$$

The branching ratio $\mathrm{Br}(\tau \to \pi^0\pi^-\nu_\tau)$ is measured to be 25.52(9)% [24]. After subtracting the 0.30(32)% non-ρ branching fraction, one has the branching fraction $\mathrm{Br}(\tau \to \rho^-\nu_\tau) = 25.22(33)\%$. Using this value along with the latest PDG2014 values of G_F, $|V_{ud}|$, m_τ, τ_τ, and m_ρ, one can get the experimental value $f_\rho^{\pm,\mathrm{exp}} = 209.4 \pm 1.5$ MeV, where the error is predominantly given by the uncertainty of the above branching fraction. Our result Eq. (11) and $f_\rho^{\pm,\mathrm{exp}}$ are in good agreement.

To summarize, we use overlap valence fermion for several quark masses on the $N_f = 2+1$ domain-wall fermion configurations generated by the RBC&UKQCD Collaboration. The light sea quark is at the physical point and the spatial extension is 5.5 fm. As a benchmark, we first calculate the decay constant of pion and obtain a value $f_\pi = 131.3(6)$ MeV at the physical pion mass, which is consistent with RBC & UKQCD's result$f_\pi = 130.2(9)$

MeV. We extract the spectrum of the $I = 1$ vector channel from the Coulomb gauge fixed wall-source correlation functions. As such the ρ mass is precisely determined to be $m_\rho = 775.9 \pm 6.0 \pm 1.8$ MeV at the physical pion mass. We also propose a strategy to reduce the noise of the wall-wall correlation functions of hadrons, through which the leptonic decay constant of ρ, f_ρ, is determined to be $208.5 \pm 5.5 \pm 0.9$ MeV at the physical m_π, which agrees well with the value $f_\rho = 209.4 \pm 1.5$ MeV derived from the process $\tau \rightarrow \rho\nu_\tau$. From the slope of m_ρ vs. m_π^2, we obtain the valence $\pi\rho$ sigma term from the Feynman-Hellman theorem which gives $\sigma_{\pi\rho}^{(\mathrm{val})} = 9.82(6)$ MeV. Future results at different lattice spacings are needed for the continuum extrapolation.

We thank the RBC&UKQCD Collaboration for providing us their DWF gauge configurations. This work is supported in part by the U.S. DOE Grant No.DE-FG05-84ER40154, and also by the National Nature Science Foundation of China (NSFC) under Grants No.11335001, No.11105153 and No.11261130311 (CRC110 by DFG and NSFC). A. A. is supported in part by the U.S. National Science Foundation under CAREER grant PHY-1151648. Y. C. thanks the support by the CAS Center for Excellence in Particle Physics (CCEPP). This research used resources of the Oak Ridge Leadership Computing Facility at the Oak Ridge National Laboratory, which is supported by the Office of Science of the U.S. Department of Energy under Contract No. DE-AC05-00OR22725.

[1] T. Blum *et al.* (RBC and UKQCD Collaborations), arXiv:1411.7017 (hep-lat).

[2] A. Bazavov *et al.* (Fermilab and MILC Collaborations), Phys. Rev. D **90**, 074509 (2014) [arXiv:1407.3772 (hep-lat)].

[3] Y.B. Yang *et al.* (χQCD Collaboration), arXiv:1410.3343 (hep-lat).

[4] M. Lujan, A. Alexandru, Y. Chen, T. Draper, W. Freeman, M. Gong, F.X. Lee, A. Li, K.-F. Liu, and N. Mathur, Phys. Rev. D **86**, 014501 (2012) [arXiv:1204.6256 (hep-lat)].

[5] A. Alexandru, M. Lujan, C. Pelissier, B. Gamari and F. X. Lee, arXiv:1106.4964 (hep-lat).

[6] R.L. Jaffe, AIP Conf. Proc. **964**, 1 (2007); Prog. Theor. Phys. Suppl. **168**, 127 (2007) [arXiv:hep-ph/0701038].

[7] J.R. Pelaez, Phys. Rev. Lett. **92**, 102001 (2004) [arXiv:hep-ph/0309292].

[8] X. Feng, K. Jansen, D.B. Renner, Phys. Rev. D **83**, 094505 (2011) [arXiv:1011.5288(hep-lat)].

[9] C. Pelissier and A. Alexandru, Phys. Rev. D **87**, 014503 (2013) [arXiv:1211.0092 (hep-lat)].

[10] S. Aoki *et al.* [CS Collaboration], Phys. Rev. D **84**, 094505 (2011) [arXiv:1106.5365 (hep-lat)].

[11] J.J. Dudek *et al.* [Hadron Spectrum Collaboration], Phys. Rev. D **87**, 034505 (2013), Phys. Rev. D **90**, 099902 (2014) [arXiv:1212.0830 (hep-ph)].

[12] M. Luscher, Commun. Math. Phys. **105**, 153 (1986).

[13] P.C. Bruns and U.-G. Meissner, Eur. Phys. J. C **40**, 97 (2005).

[14] C.W. Bernard, *et al.*, Phys. Rev. D **64**, 054506 (2001) [arXiv: hep-lat/0104002].

[15] D.B. Leinweber, A.W. Thomas, K. Tsushima and S.V. Wright, Phys. Rev. D **64**, 094502 (2001) [arXiv: hep-lat/0104013].

[16] C.R. Allton, W. Armour, D.B. Leinweber, A.W. Thomas and R.D. Young, Phys. Lett. **B 628**, 125 (2005) [arXiv: hep-lat/0504022].

[17] W. Armour, C.R. Allton, D.B. Leinweber, A.W. Thomas and R.D. Young, J. Phys. G **32**, 971 (2006) [arXiv: hep-lat/0510078].

[18] R. Lewis and R.M. Woloshyn, Phys. Rev. D **56**, 1571 (1997) [arXiv: hep-lat/9610027].

[19] A. Ali Khan *et al.* (CP-PACS Collaboration), Phys. Rev. D **65**, 054505 (2002) [arXiv: hep-lat/0105015].

[20] M. Gockeler, R. Horsley, D. Pleiter, P.E.L. Rakow, G. Schierholz, W. Schroers, H. Stüben, and J.M. Zanotti, Proc. Sci. LAT **2005**, 063 (2006) [arXiv: hep-lat/0509196].

[21] K. Hashimoto and T. Izubuchi, Prog. Theor. Phys. **119**, 599 (2008) [arXiv:0803.0186 (hep-lat)].

[22] K. Jansen, C. McNeile, C. Michael, and C. Urbach (ETM Collaboration), Phys. Rev. D **80**, 054510 (2009) [arXiv:0906.4720 (hep-lat)].

[23] Z. Liu, Y. Chen, S.-J. Dong, M. Glatzmaier, M. Gong, A. Li, K.-F. Liu, Y.-B. Yang, and J.-B. Zhang (χQCD Collaboration), Phys. Rev. D **90**, 034505 (2014) [arXiv:1312.7628 (hep-lat)].

[24] K.A. Olive *al.* (Particle Data Group), Chin. Phys. C **38**, 090001 (2014).